Aero 48-88

Department of AERONAUTICS and ASTRONAUTICS
STANFORD UNIVERSITY

Final Report to
NASA-Ames Research Center

SHOCK TUBE INVESTIGATION OF DYNAMIC RESPONSE OF PRESSURE TRANSDUCERS FOR VALIDATION OF ROTOR PERFORMANCE MEASUREMENTS

NASA Reference NCC 2-549

Submitted by
Professor Daniel Bershader
Department of Aeronautics and Astronautics
Stanford University
Stanford, California 94305-4035

December 1988

Background and Orientation

For some time now, NASA has had a program under way to aid in the validation of rotor performance and acoustics codes associated with the UH-60 rotary-wing aircraft; and to correlate results of such studies with those obtained from investigations of other selected aircraft rotor performance. A central feature of these studies concerns the dynamic measurement of surface pressure at various locations up to frequencies of 25 KHz. For this purpose, fast-response gauges of the Kulite type are employed. The latter need to be buried in the rotor; they record surface pressures which are transmitted by a pipette connected to the gauge. The other end of the pipette is cut flush with the surface. In certain locations, the pipette configuration includes a rather sharp right-angle bend. The natural question has arisen in this connection: In what way are the pipettes modifying the signals received at the rotor surface and subsequently transmitted to the sensitive Kulite transducer element?

This problem is especially well-suited to the application of shock tube techniques with which pressure step functions can be applied to the gauge and the results monitored. The present report contains the basic details and results of the program performed and recently completed in the High Pressure Shock Tube Laboratory of the Department of Aeronautics and Astronautics at Stanford University.

Overview of the Program

As indicated above, this study is concerned with the design and implementation of a series of shock tube experiments to quantify the frequency response of combined Kulite gauge-pipette configuration, orientation with respect to shock direction, and shock strength as parameters. Passage of a shock wave of known strength over the test configuration produced a response which was presented on a pressure-time plot. Results were obtained for various lengths of pipette. Relatively weak shocks were generated for these experiments, in order to stay within the linear region of the gauge response; this limitation was also in accordance with the wishes of the NASA-Ames sponsors. The basic results, namely the pressure-time plots representing the

response of the various configurations, are included in this report.

Major Aspects of the Experiments

The simplest and most convenient device for producing controlled shocks is a shock tube. For a simple shock tube using room temperature air in the driver section and room temperature air at atmospheric pressure in the test section, the strength of the shock is determined by the initial pressure in the driver section. The pressure in the driver section of the shock tube required to produce a pressure jump of a given magnitude is easily calculable from the Taub equation:

$$\frac{P_4}{P_1} = \frac{P_2}{P_1}\left[1 - \frac{(\gamma-1)(P_2/P_1 - 1)}{(2[(\gamma+1)(P_2/P_1 - 1) + 2])^{1/2}}\right]^{\frac{-2\gamma}{\gamma-1}}$$

where P_1 = pressure in the test section
P_2 = pressure behind the shock
P_4 = pressure in the driver section
γ = ratio of specific heats of test and driver gases
$P_2 - P_1$ = pressure step magnitude

The Stanford High Pressure Shock Tube utilizes a test section whose cross section is 2.00" x 2.00" (or 5.0 cm x 5.0 cm), consisting of extruded aluminum .75" in thickness. The test configuration is inserted with end of pipette flush with the side of the test section. Figure 1a is a schematic diagram showing principal features of the experimental arrangement. Components include (1) high-pressure air supply for the driver, (2) laser-counter system for measuring shock velocity (therefore shock strength); (3) pressure transducer test configuration with amplifier, digital oscilloscope and plotter; and, of course (4) the shock tube itself. Details of the overall gas manifold and control panel with pressure gauges have been omitted, as have the power supply for the Kulite gauge.

The test section of the shock tube is many diameters away from the diaphragm to allow full development of the shock before the shock reaches the test section. A pressure jump of 5 psi over atmospheric is

desired to remain well within the linear response range of the transducer. After substitution of the desired values for the pressure jump and solution of the Taub equation, an overpressure of 12 psi is found to be required in the driver section. For such low pressure differences a very thin diaphragm is needed. Some of the standard diaphragms used for such purposes are of aluminum foil or acetate. By trial and error it was found that Reynolds Heavy Duty Aluminum Foil would spontaneously burst at an overpressure of approximately 11 psi in the driver section, making it a satisfactory choice.

The speed of the shock provides a more accurate indicator of the pressure jump across the shock than the burst pressure of the diaphragm. The two laser shock-detecting stations are spaced 0.60m apart. Each station consists of a pair of windows in the shock tube which create an optical path for an 0.8mW HeNe laser beam to pass through the tube. After passing through the tube, the laser beam is incident on a photodiode which in turn is connected to an amplifying circuit. As the shock passes each detecting station, the laser beam is diverted from the photodetector by refractive index gradients in the passing shock, creating a trigger pulse which is amplified. The time between the two trigger pulses is measured by a 10 MHz counter, thereby providing a measure of shock speed.

The test section of the shock tube consists of a pair of opposing round ports, 3.0" in diameter which are normally fitted with quartz windows for optical measurements. For the pressure transducer measurements, one window was removed and a specially designed plug, 0.75 in. thick was fitted to the port. A small hole was drilled through the core of the plug and the pipette of the pressure transducer was fitted snugly in the hole. The body of the transducer was then affixed to the outside of the plug with cyanoacrylate ester. After the measurements at a given length of pipette were made, the plug was removed from the shock tube, and the measurement face was cut 0.125" on a lathe. After each cut, the end of the pipette was carefully deburred and inspected. The plug was then remounted in the shock tube and further measurements made. Fig. 1b shows a schematic of the transducer-pipette assembly mounted in the shock tube wall.

The basis of the Kulite pressure transducer itself consists of a

four-arm Wheatsone Bridge plated onto the surface of a silicon diaphragm. The arms of the Wheatstone Bridge act like strain gauges, measuring the strains in the diaphragm caused by pressure differentials as changes in resistance. An external power supply holds a constant voltage across the Bridge so that the changes in resistance can be measured as a current signal which is amplified by an external unit. Within the range of the transducer the strains in the diaphragm increase linearly with increasing pressure differential, the resistance of the arms of the Wheatsone Bridge change linearly with strain, and, by Ohm's law, the current gives a linear measure of resistance at constant voltage. In this way, the current signal from the transducer provides a linear measure of the pressure differential across the diaphragm.

The Kulite pressure transducer is connected to a Pacific Precision Power Supply and Amplifier unit which provides both the 5V excitation voltage and the signal amplification required by the transducer. The output signal is sent to a Gould digital oscilloscope set to a 25% pretrigger. A hard copy of the trace is then provided by a Hewlett Packard plotter which interfaces with the Gould oscilloscope via a GPIB cable.

For each pipette length, three measurements were made. Two of the measurements were superimposed on a time scale long enough to show the signal to steady state and another measurement was made on a shorter time scale to achieve better resolution for the measurement of the rise time. The two measurements on the longer time scale are intended to demonstrate the reproducibility of the measurements.

For these experiments to be meaningful, it is, of course, important that the rise time of the input step be much shorter than the characteristic gauge response time; or that the characteristic frequencies have the opposite ratio. For a gauge diameter of .012" (.305 mm), the transit time for a shock travelling at 1.55×10^4 inches/sec (.346 mm/μsec) is .77 μsec, corresponding to a frequency of 1.29 Megaherz. The latter figure is appreciably higher than characteristic gauge response times -- a satisfactory situation.

Presentation of Results

The basic results are contained in the plots of output voltage vs. time, as given in Figs. 2 through 9. The figures show 2 plots each, in accordance with an earlier remark about verifying the reproducibility of the data. The curves represent output in millivolts vs. time in microseconds after shock excitation. Succeeding graphs represent sequentially shorter pipette lengths in steps of 1/8", except at the very short end; the last two cuts were 1/16" and 1/36", respectively. The millivolt output is convertible to pressure amplitude, since the asymptotic (D.C.) pressure rise, in the range close to 4.6 psi, is given to three significant figures on each graph. The corresponding voltage is measurable on the plot, thus permitting the conversion. Thus, for example, in Fig. 2 one division of 500 mV corresponds to a pressure change of 1.47 psi.

A second series of runs were made with the recording time scale expanded by a factor of 4, from 200 μsec per division to 50 μsec per division. The corresponding plots are given in Figures 10 through 17.

The final set of results are those for an unmodified Kulite transducer 3/32 in. diameter (see Fig. 18). The results are shown graphically in Figures 19 and 20. The last plot, Fig. 21, shows background noise and is included for reference. It consists of a "spikey" 60-cycle disturbance of about 25 mV amplitude, corresponding to about .07 psi.

Assessment

From the plots starting with Fig. 2, it is evident that the addition of the pipette yields a vibrating system with damping which can be analyzed in terms of lumped parameters. The decaying oscillations show that the motion is underdamped. The damping is due to viscous resistance impeding the oscillating fluid motion.

As an approximate check of this modeling, a simplified calculation was made for the natural frequency (or period). It was assumed that the straight portion of the pipette corresponded to the neck of a Helmholtz resonator; and the total volume included also the right angle section, plus the volume immediately adjacent to the face of the

transducer. The calculated period is given by

$$T = \frac{2\pi}{c}\sqrt{\frac{LV}{A}},$$

where L is as shown in Fig. 1b
A is cross-sectional area of pipette
V is the total volume
c is the velocity of sound

The numerics give T = 498 μsec ± 10%.

Measurements of the first two periods of the damped oscillation on Fig. 2 give T = 440 μsec. Considering the uncertainties, e.g., the difficult-to-determine volume at the transducer face, the agreement is felt to be quite good. Of course, a more exact calculation would take into account the effect of damping on frequency, but that was not felt to be necessary here.

Turning to the damping, we may define the usual logarithmic damping factor δ, given here by

$$\delta = \frac{4\pi^2\nu}{c}\sqrt{\frac{LV}{A^3}},$$

where υ = kinematic viscosity = 0.0233 in^2/sec for air. The calculated result is δ = 0.644. Since δ is the natural log of the ratio R of two successive peaks (half-period), we find that R = 1.90.

Measurements on Fig. 2 give an average value R = 2.00. Here again, the agreement is quite good, yielding a verification of the model within the modest precision of these determinations.

Comparison of successive records starting with Fig. 2 shows that the energy in the damped oscillations decreases markedly with the decrease in the L-dimension. Note in Fig. 2 that the "ringing" lasts for about 1 millisecond. When L is reduced by .125" (Fig. 3), the ringing decreases to about 0.6 milliseconds. After another .125" cut, the time

is further reduced to about 0.4 millisec. And so on.

Returning to Fig. 2, one can observe an initial transient rise time before commencement of the damped oscillation. Its value is about 100 μsec. Note that this feature does not change significantly with the shortening of the pipette.

Another feature concerns some additional background noise superimposed on the steady-state signal when L becomes quite short. Thus, compare Fig. 4 (L = 0.500 in) with Fig. 9 (L = 0.035 in). Evidently, when the distance of the pipette orifice from the right-angle bend reaches just a few tube diameters, account has to be taken of the more complex geometry. The complexity probably shows up in the modal patterns, including any effects of phase.

The time-expanded data, starting with Fig. 10 show a nearly undamped high-frequency ringing of quite small amplitude. The frequency is approximately 240 KHz, which is just in the range of the natural frequency of these gauges as reported in the Kulite specifications in their catalog.

Turning now to the unmodified 3/32" Kulite gauge, we see from the plots in Figs. 19 and 20 two significant features, namely (1) rise time and (2) ringing frequency. The former is about 20 μseconds, while the frequency is about 108 KHz, again closely in line with what Kulite reports for its --093 series of gauges at these modest overpressures. However, the amplitude of the ringing of this "bare" gauge is appreciable, namely .85 psi peak-to-peak, approximately 18% of the 4.8 psi pressure rise across the shock. In retrospect, it was felt that this gauge is designed for larger pressure loads, but the exact model number was not available at the time of the preparation of this report.

Summary

Transient response tests were run on two Kulite gauges, one modified by a pipette connection whose length was sequentially changed during the test series.

The results obtained verified that the modified gauge presented an underdamped response whose frequency and damping constant essentially agreed with calculations based on a lumped-parameter Helmholtz resonator model. Results were obtained for the rise time, and the background noise as well.

The unmodified gauge (but a different Kulite model) showed no such characteristic damping. Its rise time was shorter but the amplitude of its natural ringing frequency was relatively large in comparison to the pressure jump of the energizing shock.

Acknowledgments

Most of the experimental work was performed by Walter Gillespie, and his assistance is gratefully acknowledged. The suggestions and assistance of Professor Michael Mandella of San Jose State University were most helpful as well.

Schematic of Shock Tube Configuration for Testing Transient Response of Modified Kulite Pressure Transducers

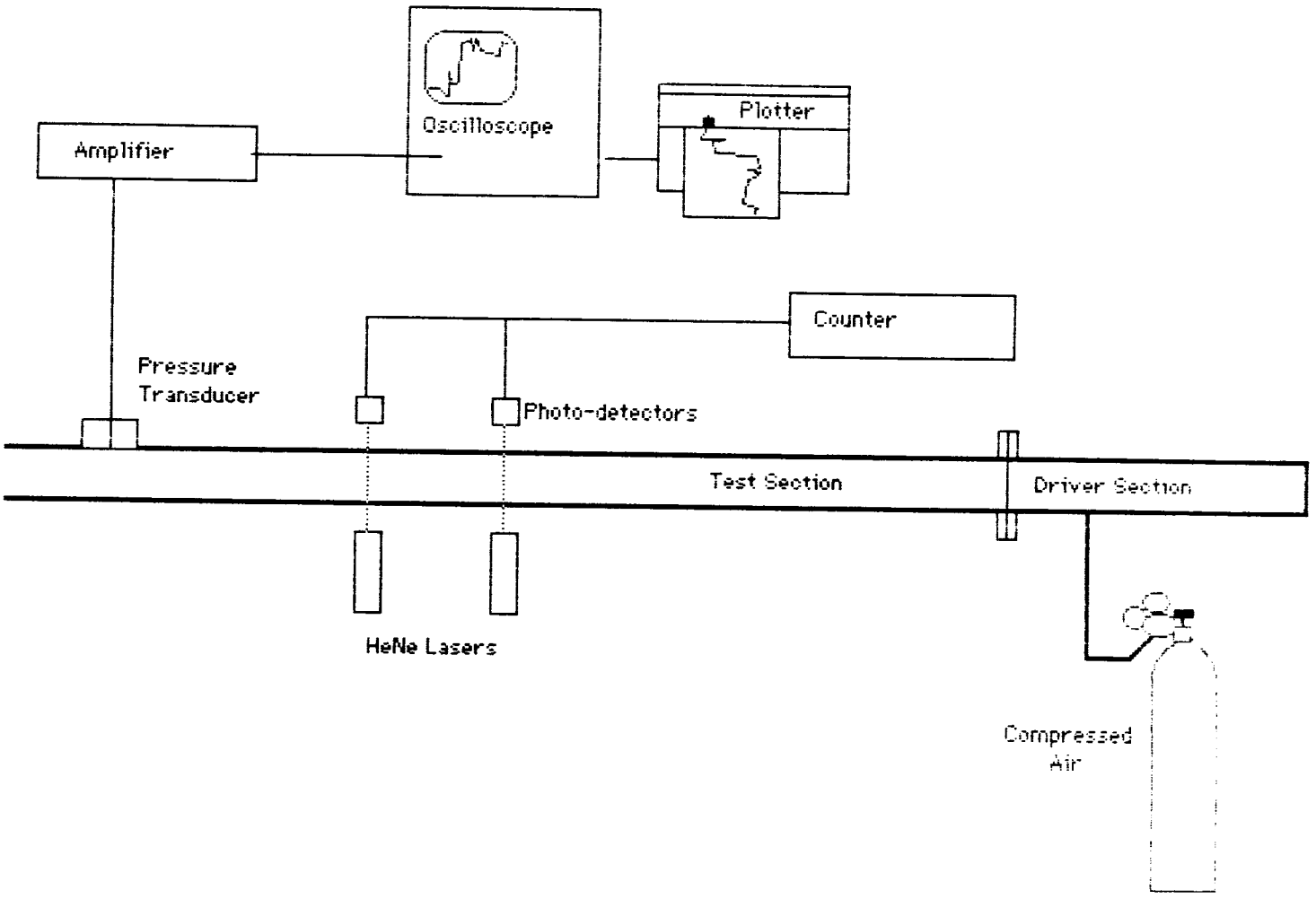

Fig. 1a

Schematic diagram of the 1/16" Kulite Pressure
Transducer-pipette Assembly Mounted in the Shock Tube.
Tests were run at lengths L ranging between 0.035 to .750 in.

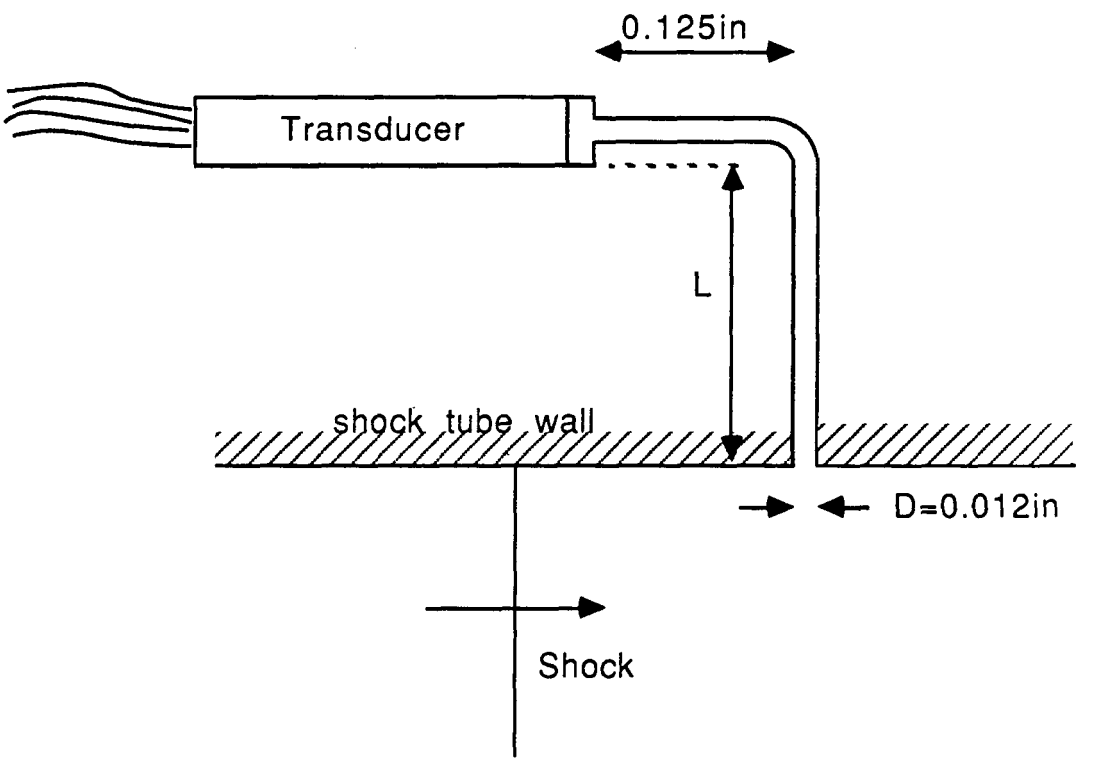

Fig. 1b

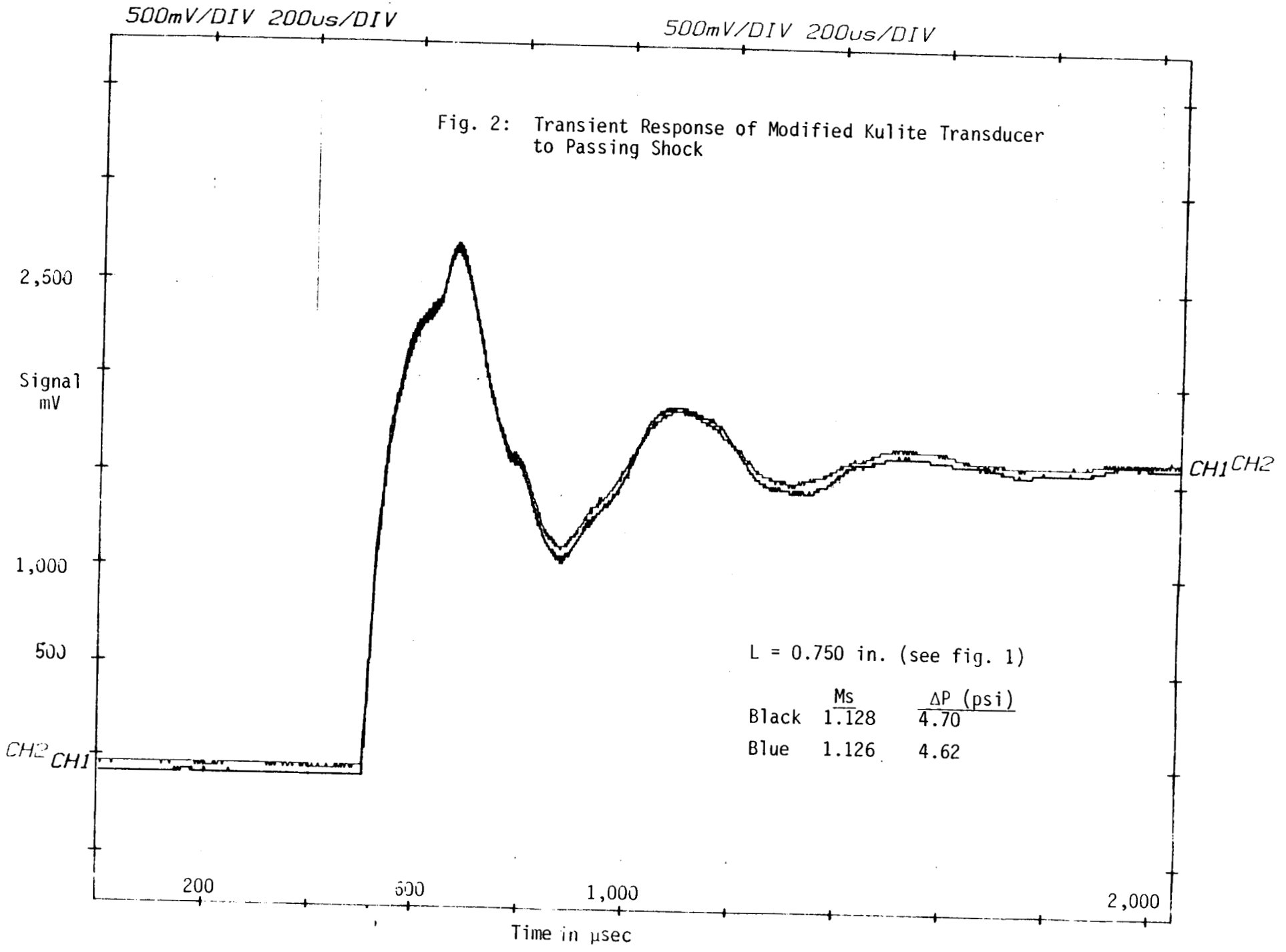

Fig. 2: Transient Response of Modified Kulite Transducer to Passing Shock

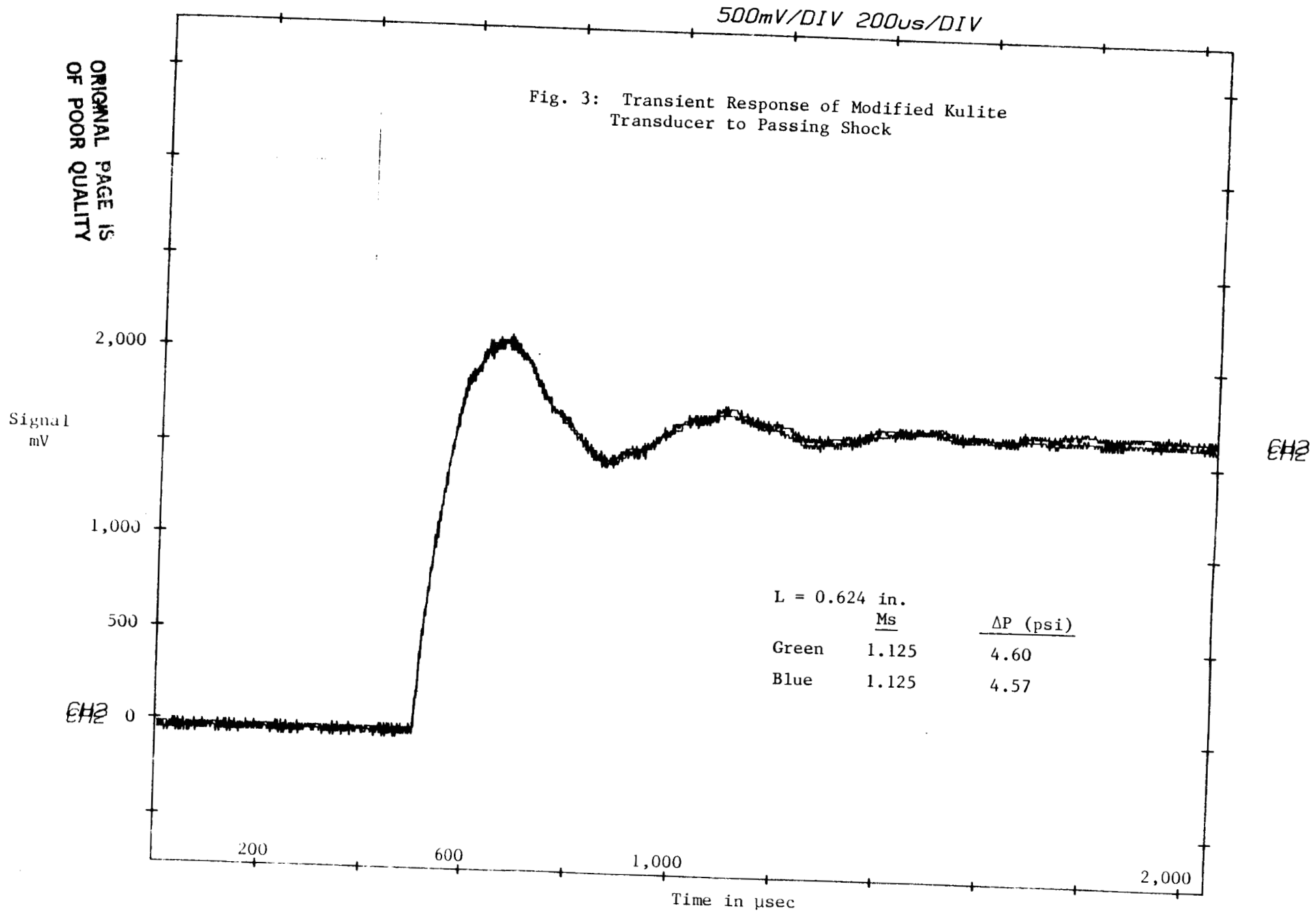

Fig. 3: Transient Response of Modified Kulite Transducer to Passing Shock

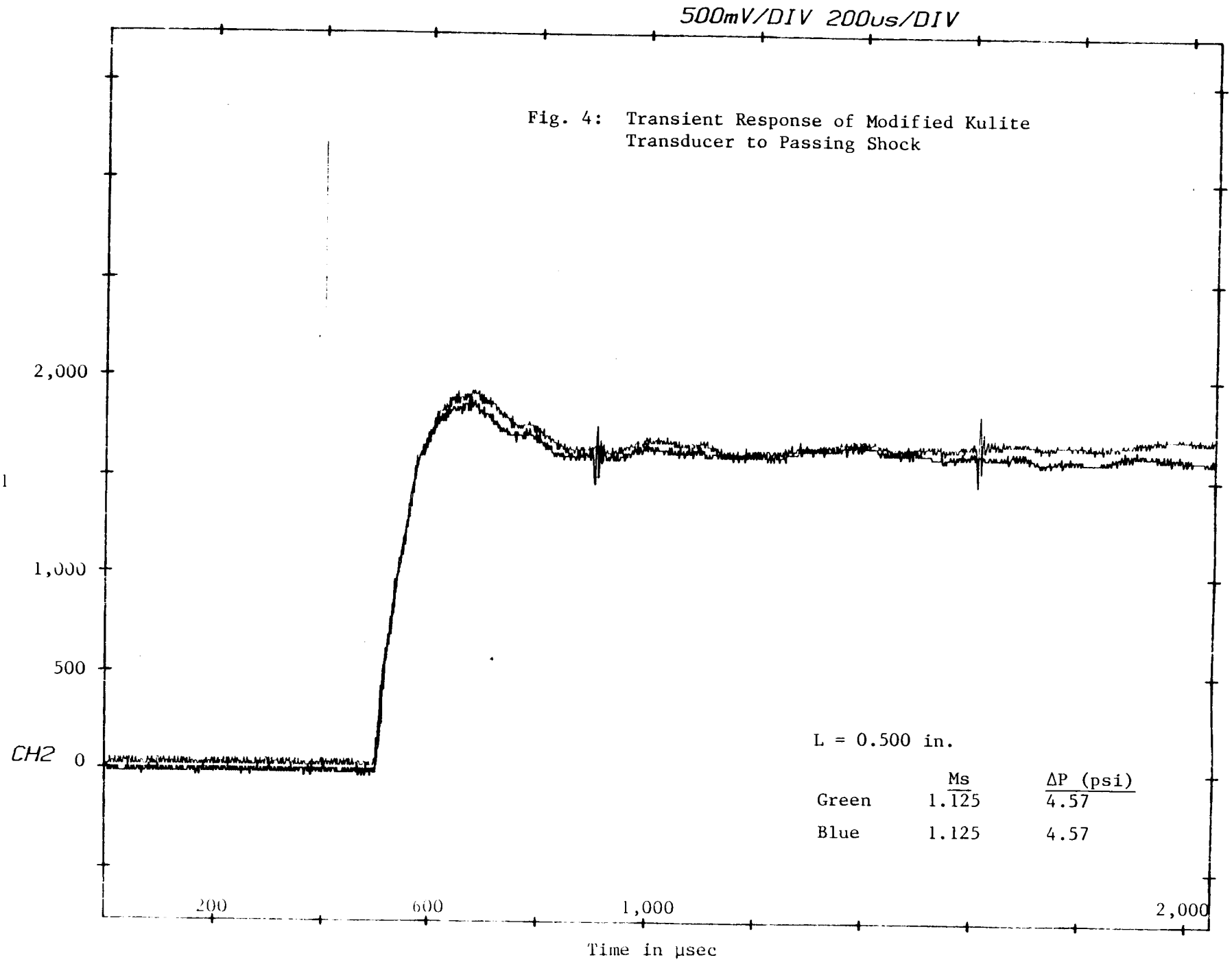

Fig. 4: Transient Response of Modified Kulite Transducer to Passing Shock

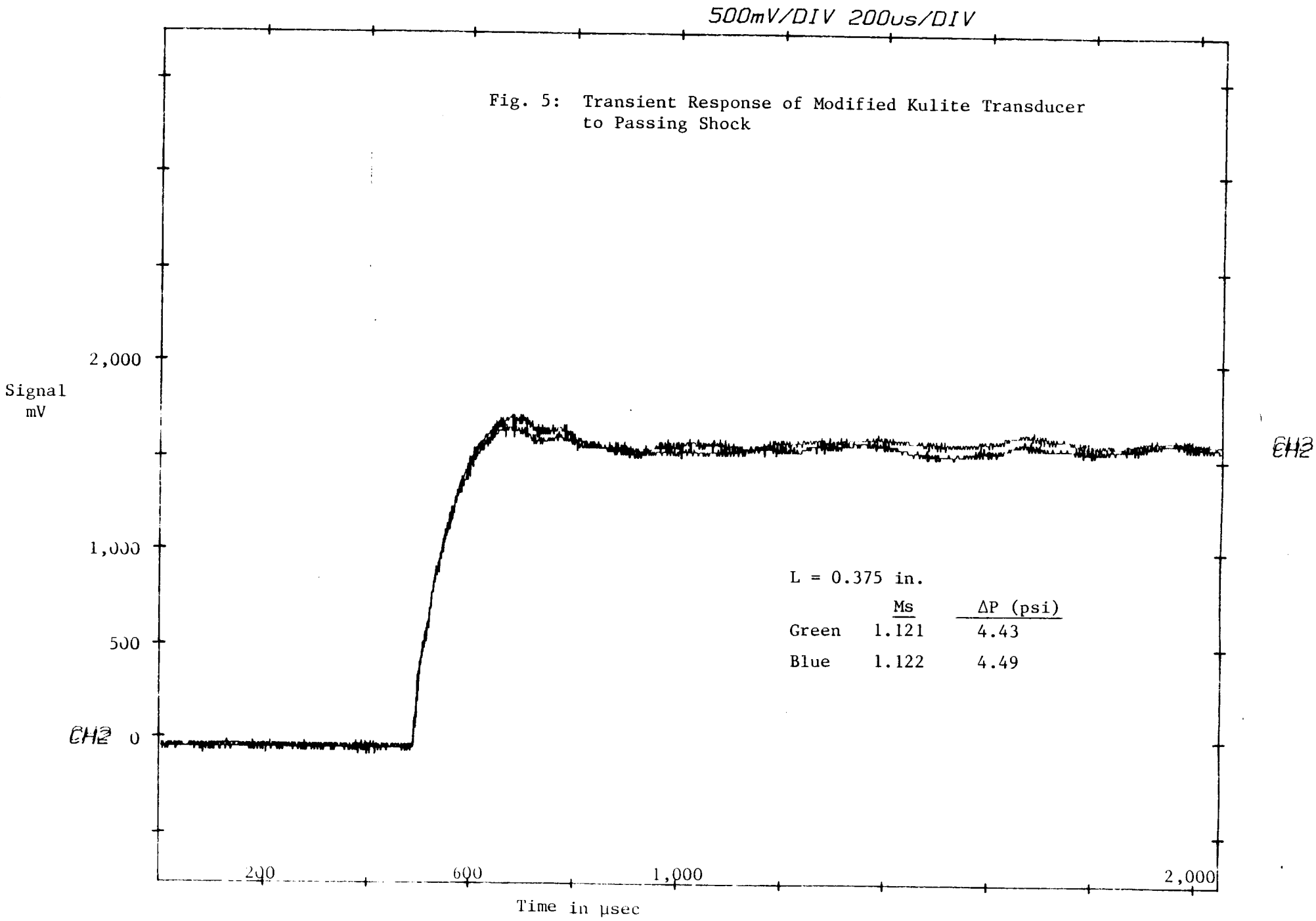

Fig. 5: Transient Response of Modified Kulite Transducer to Passing Shock

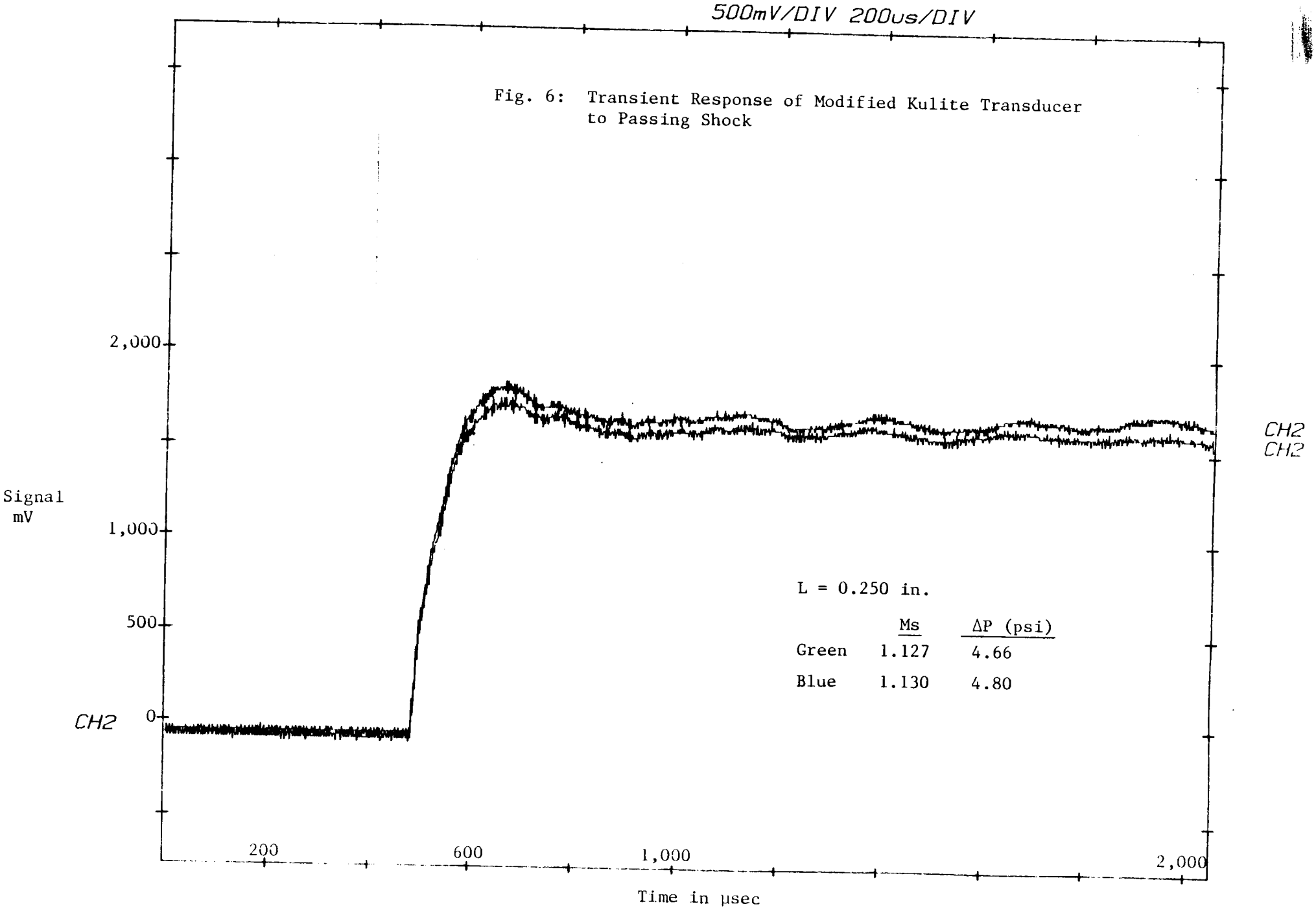

Fig. 6: Transient Response of Modified Kulite Transducer to Passing Shock

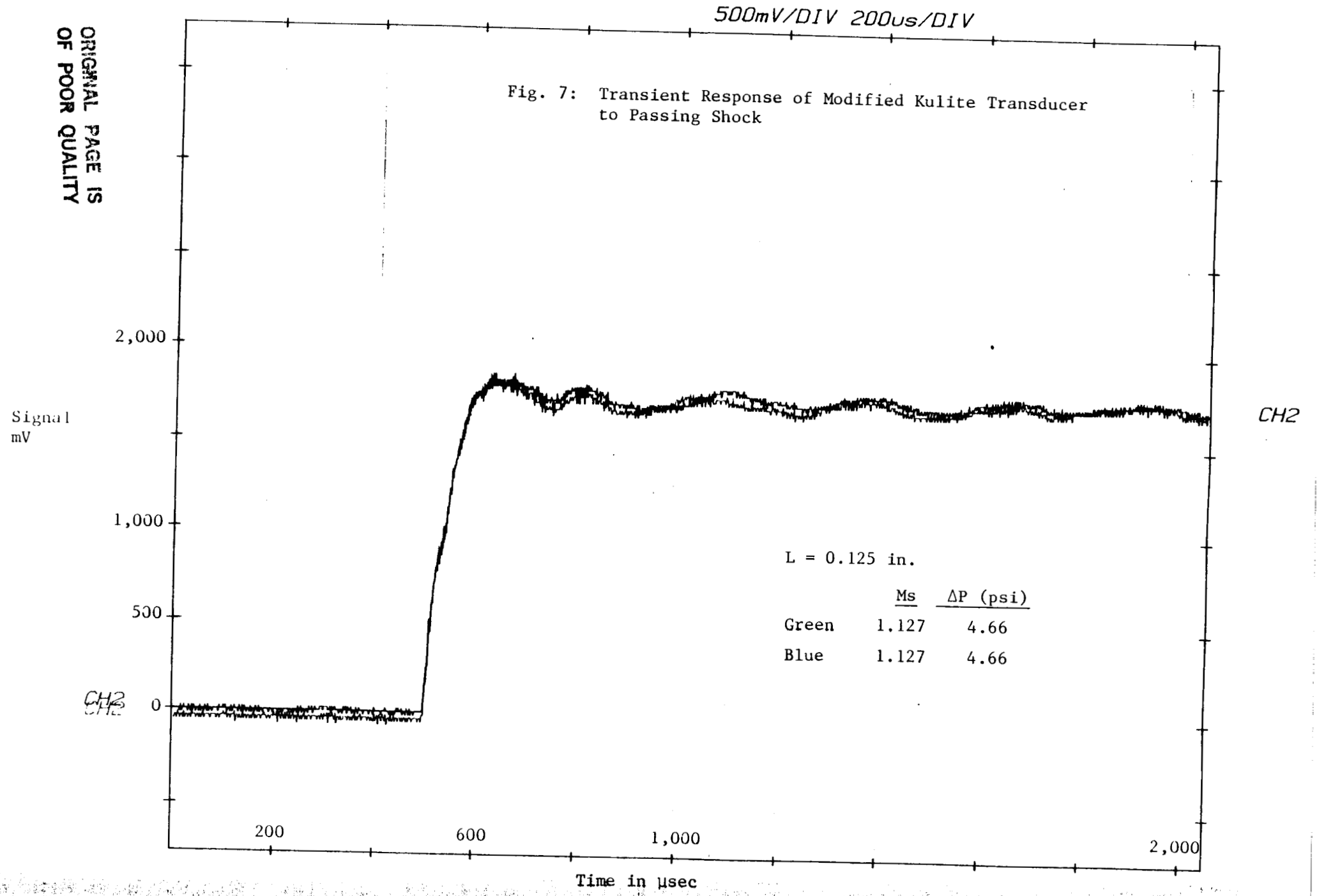

Fig. 7: Transient Response of Modified Kulite Transducer to Passing Shock

L = 0.125 in.

	Ms	ΔP (psi)
Green	1.127	4.66
Blue	1.127	4.66

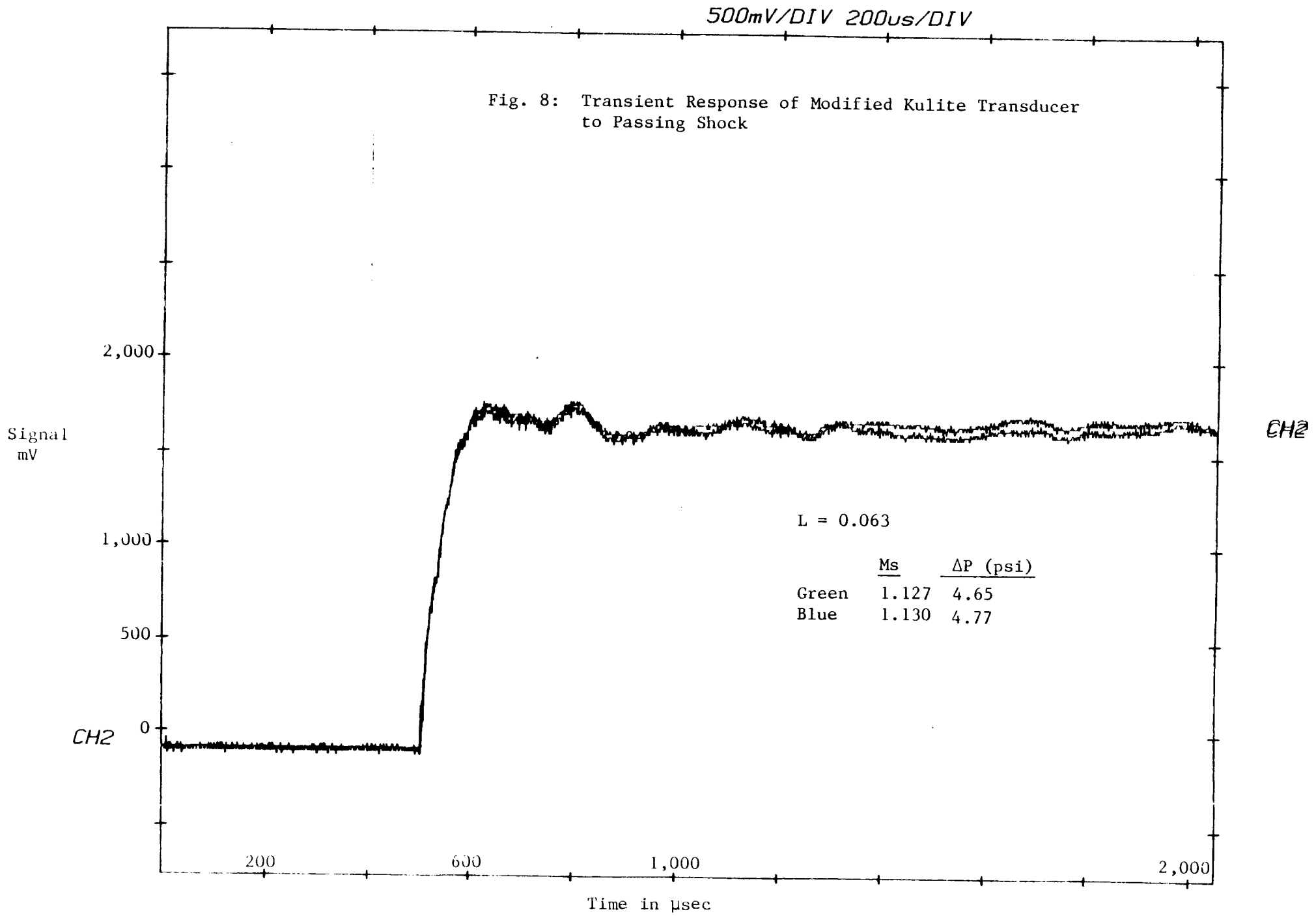

Fig. 8: Transient Response of Modified Kulite Transducer to Passing Shock

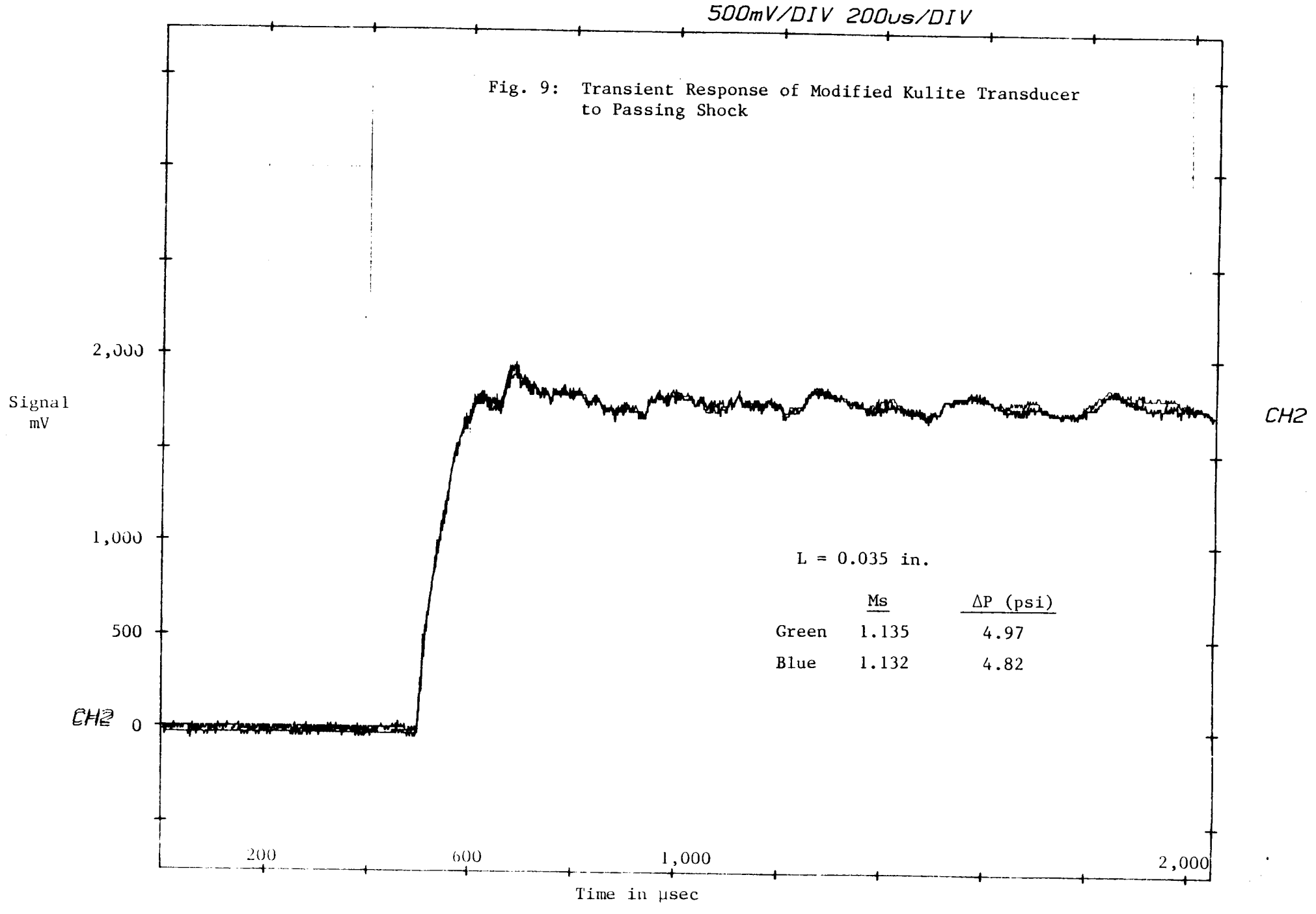

Fig. 9: Transient Response of Modified Kulite Transducer to Passing Shock

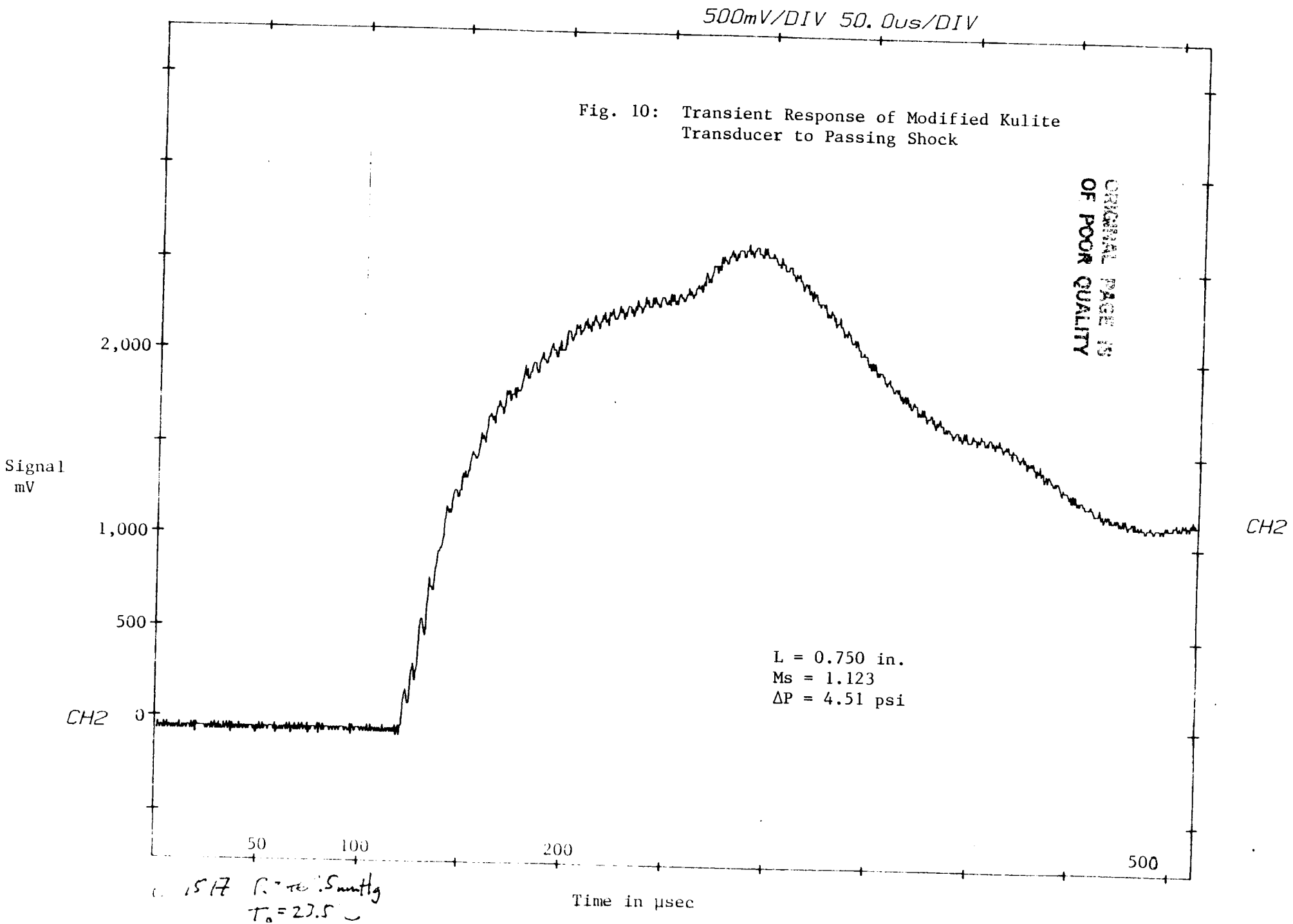

Fig. 10: Transient Response of Modified Kulite Transducer to Passing Shock

1517 Ro = .5 mmHg
T_o = 23.5

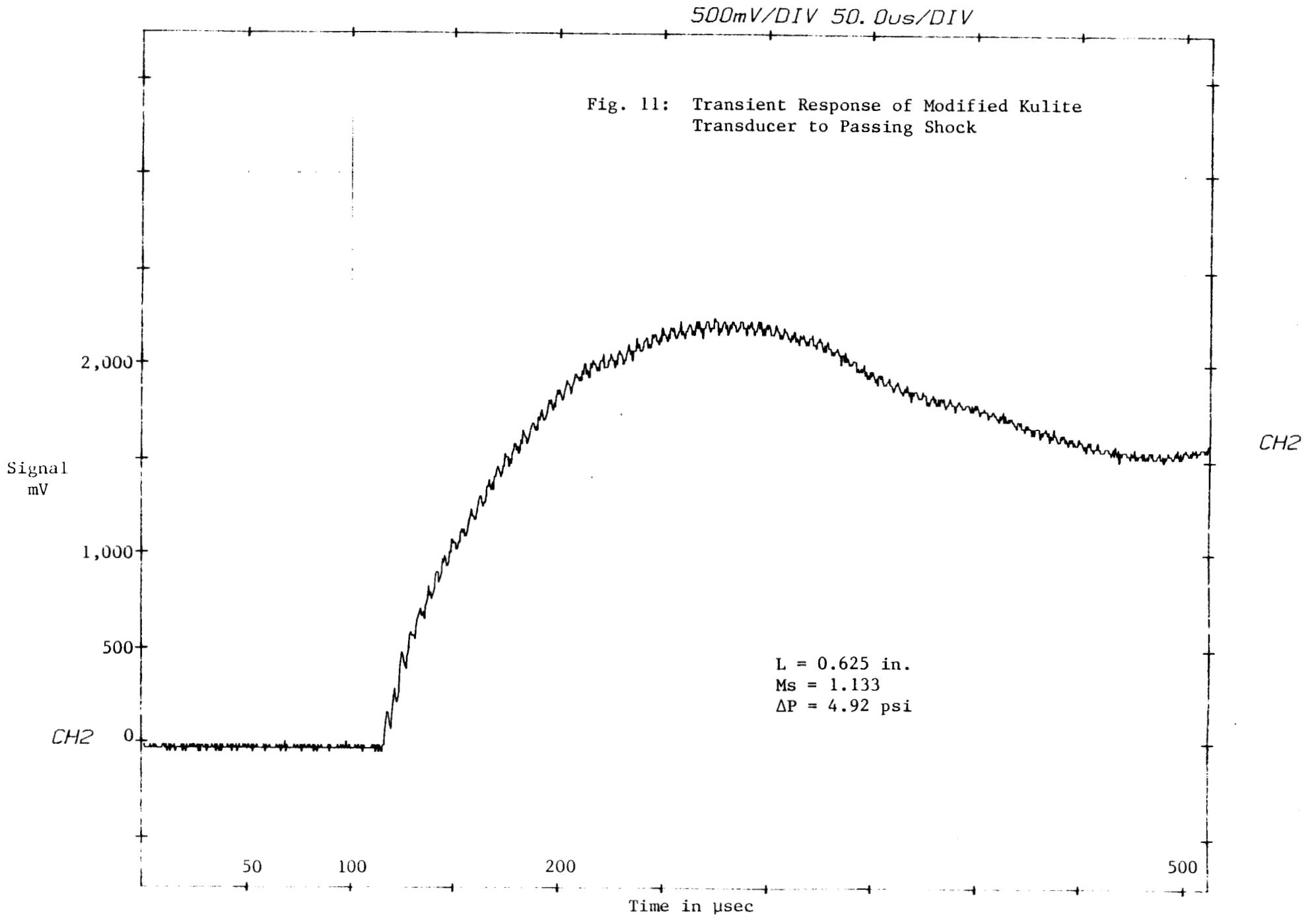

Fig. 11: Transient Response of Modified Kulite Transducer to Passing Shock

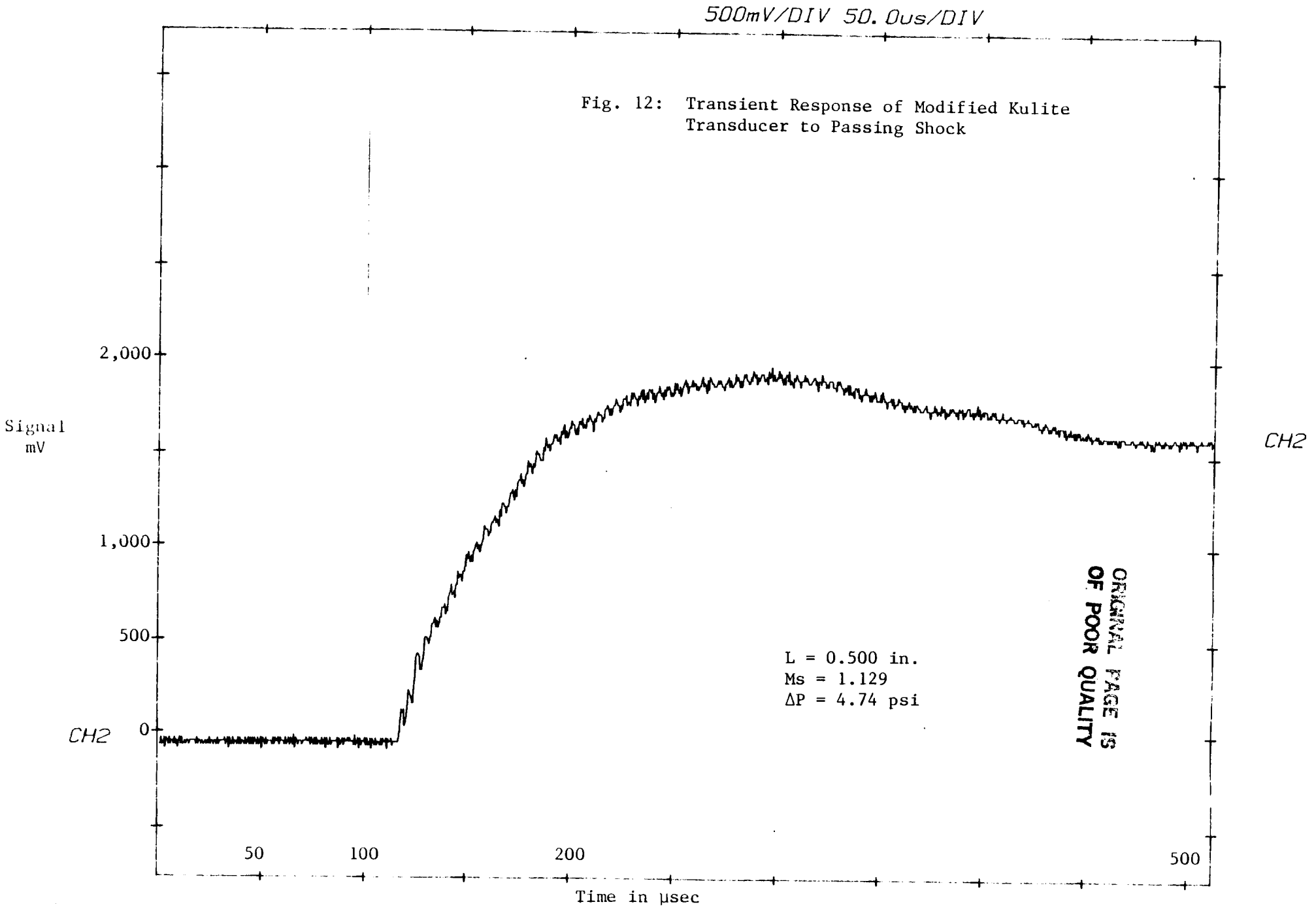

Fig. 12: Transient Response of Modified Kulite Transducer to Passing Shock

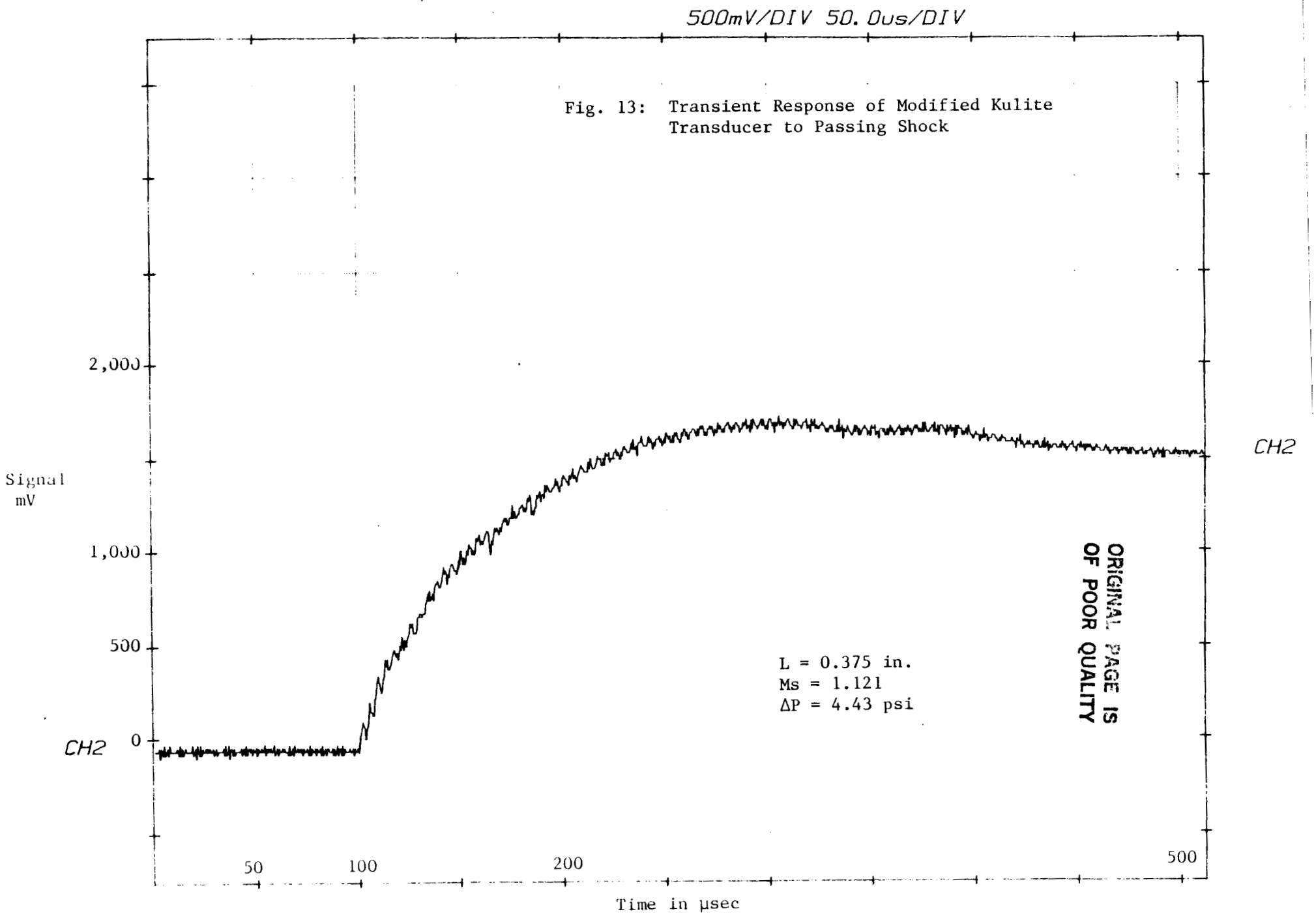

Fig. 13: Transient Response of Modified Kulite Transducer to Passing Shock

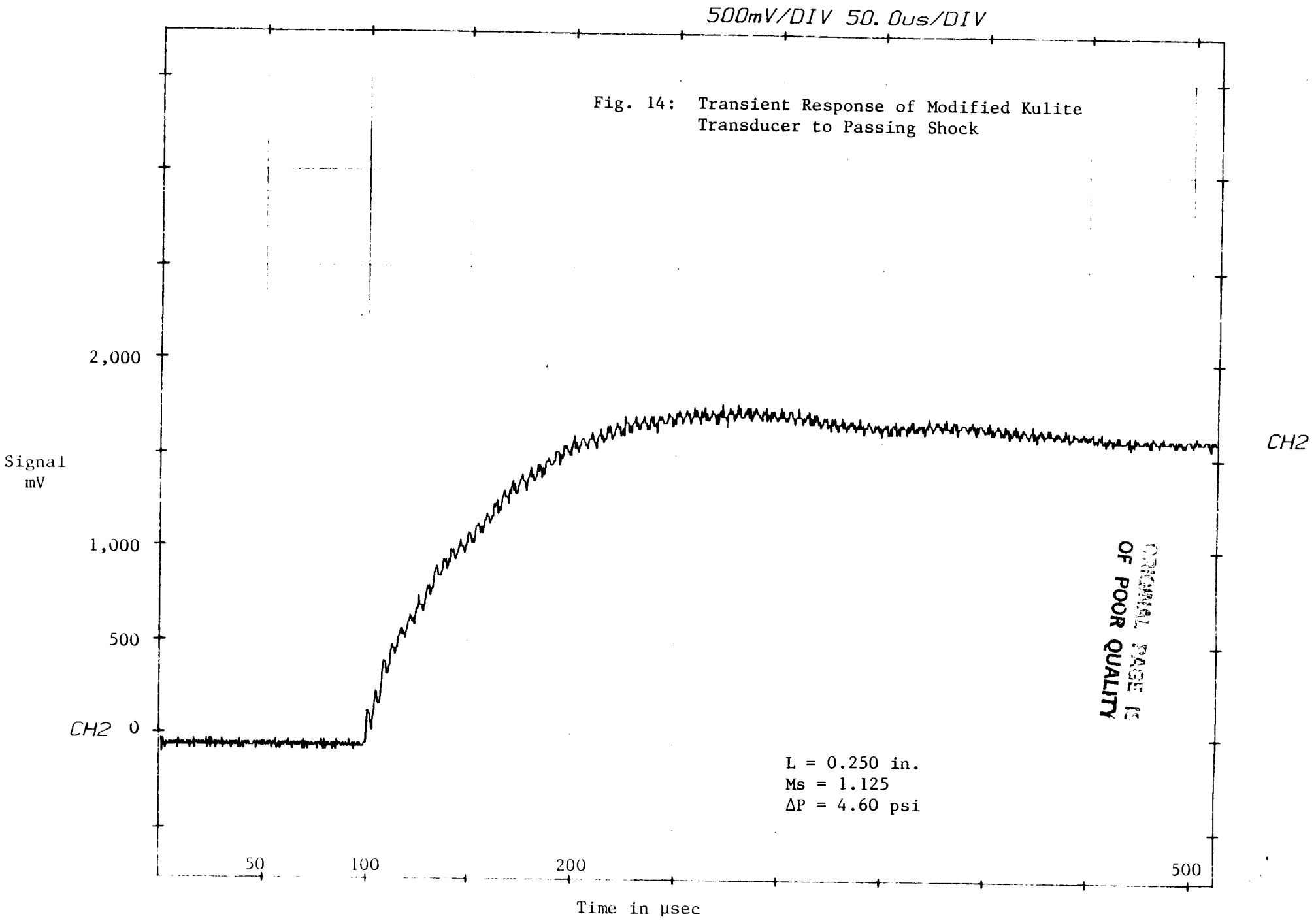

Fig. 14: Transient Response of Modified Kulite Transducer to Passing Shock

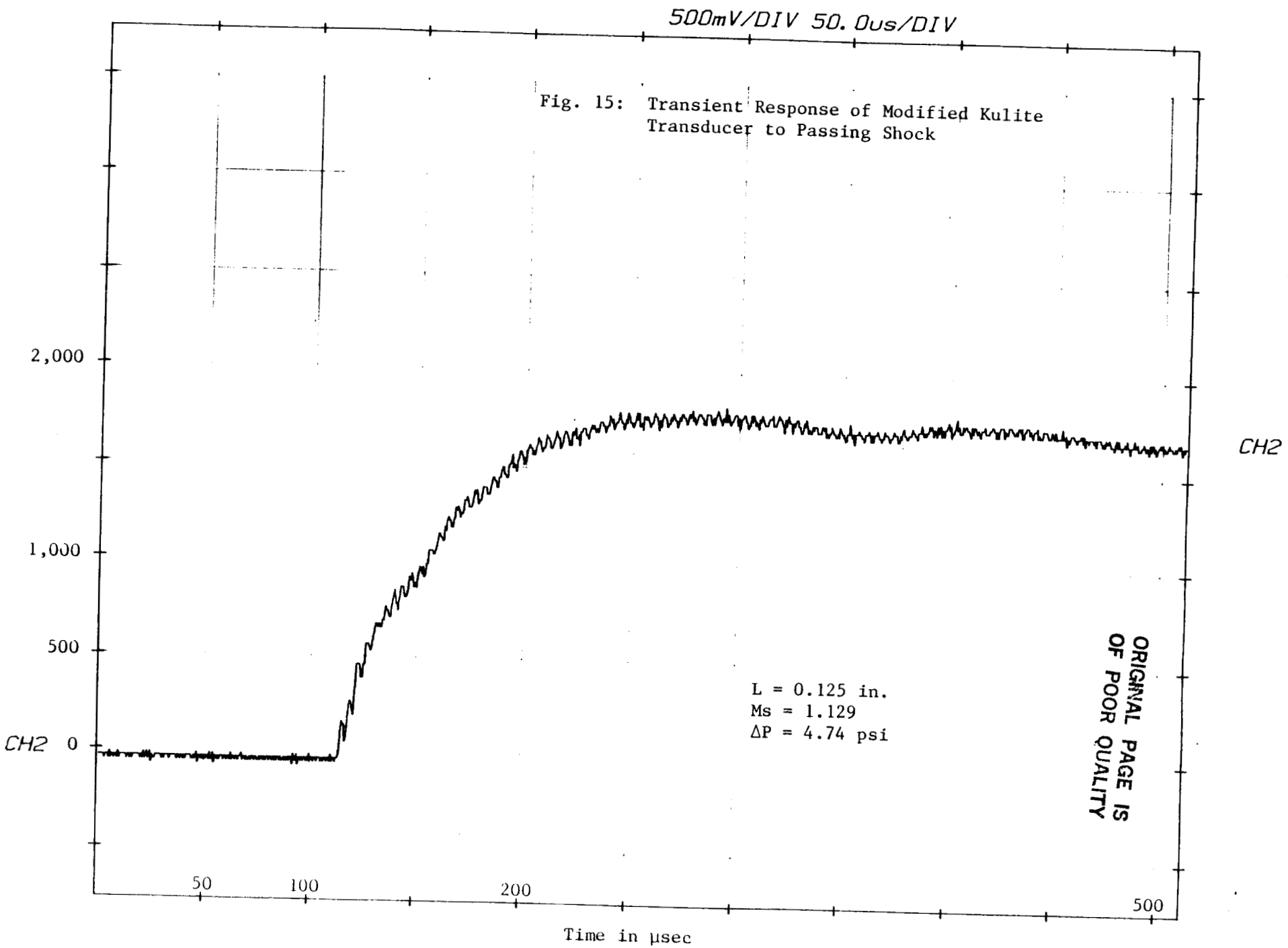

Fig. 15: Transient Response of Modified Kulite Transducer to Passing Shock

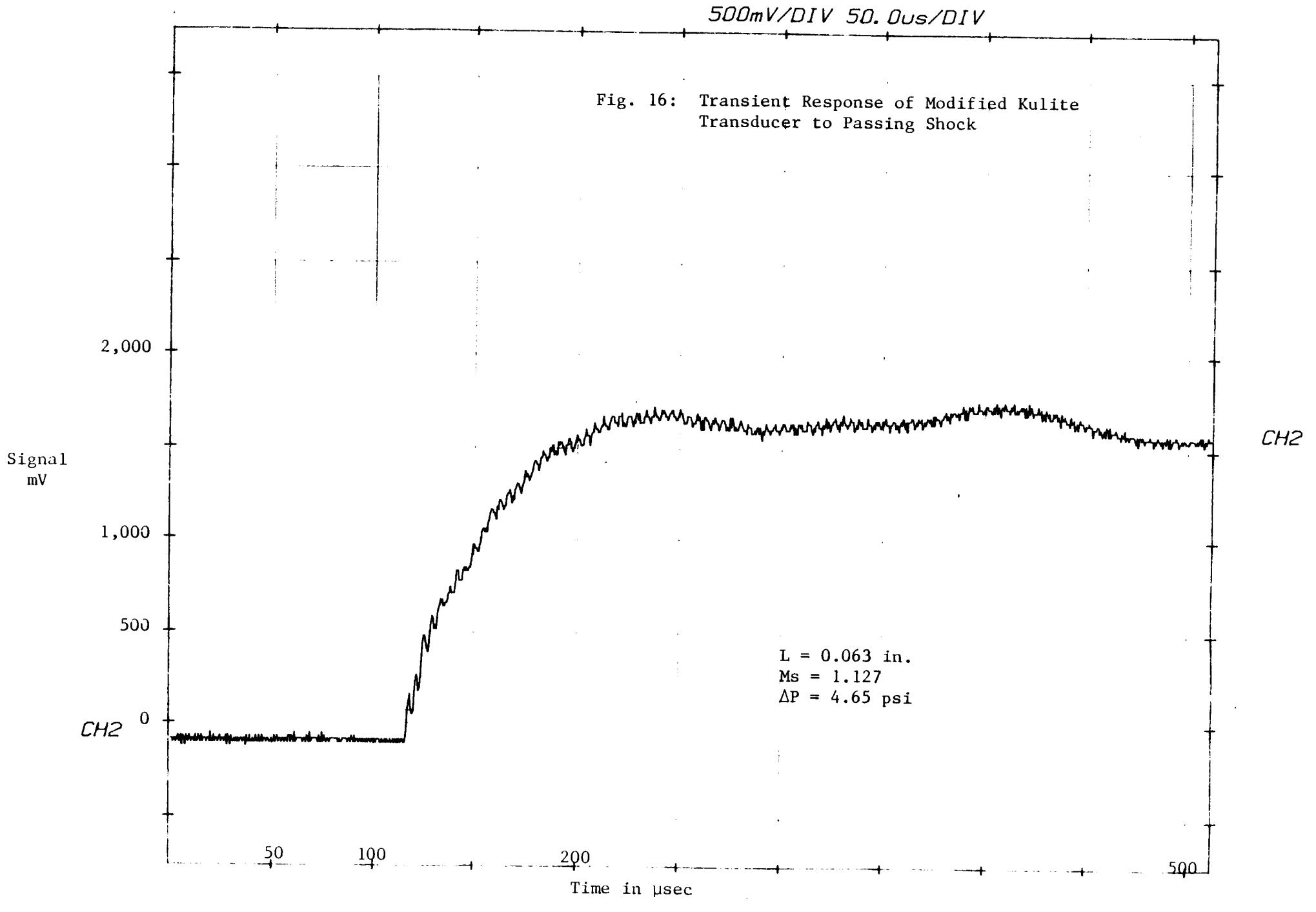

Fig. 16: Transient Response of Modified Kulite Transducer to Passing Shock

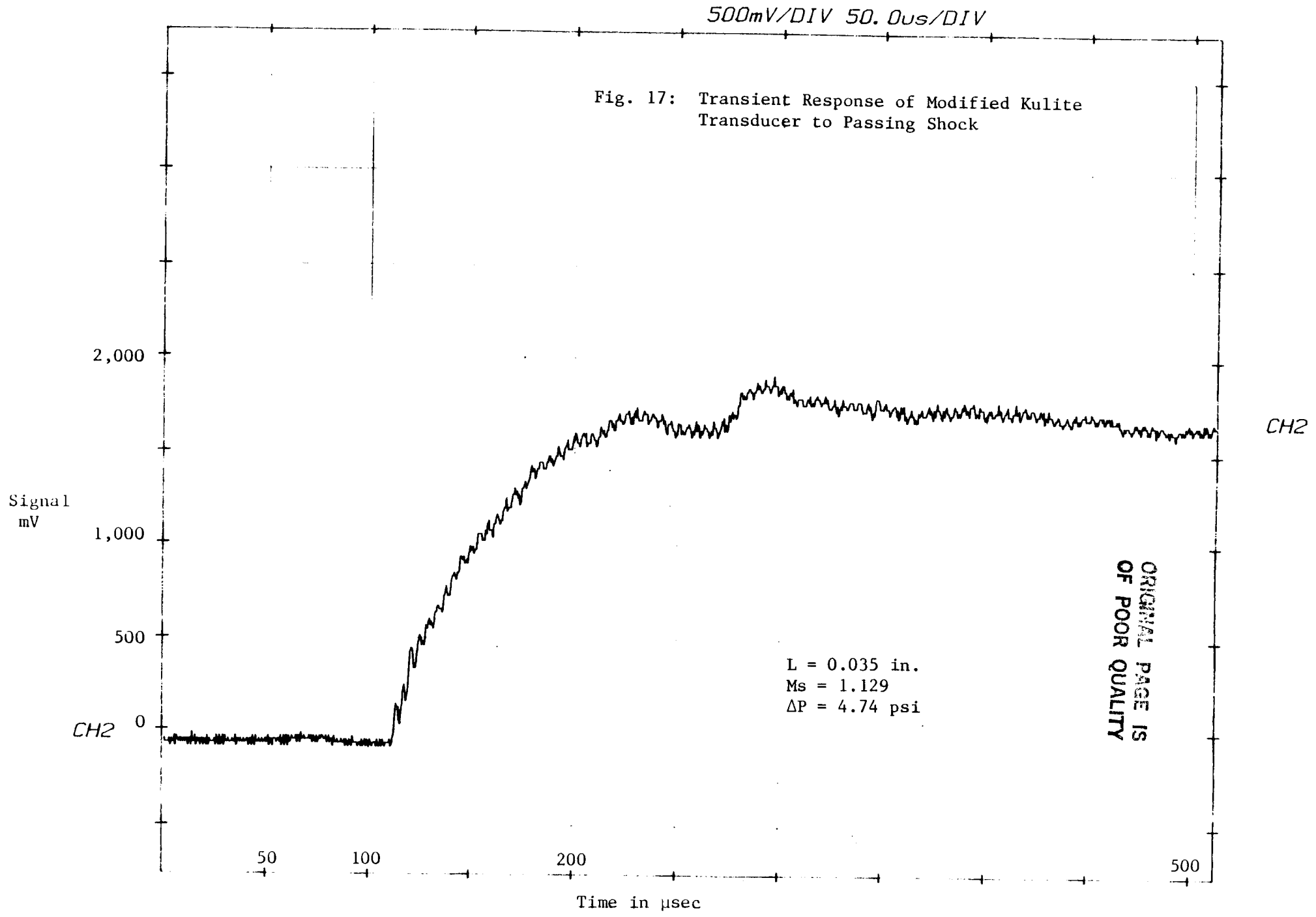

Fig. 17: Transient Response of Modified Kulite Transducer to Passing Shock

Schematic Diagram of the 3/32" Kulite Pressure
Transducer (No Pipette Attachment) Mounted in Shock Tube

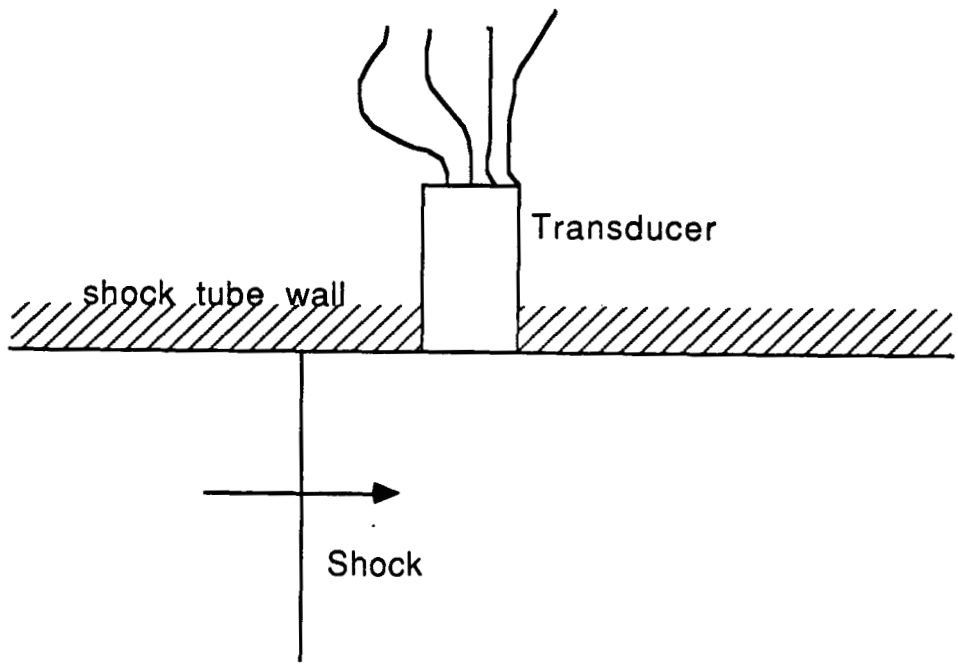

Fig. 18

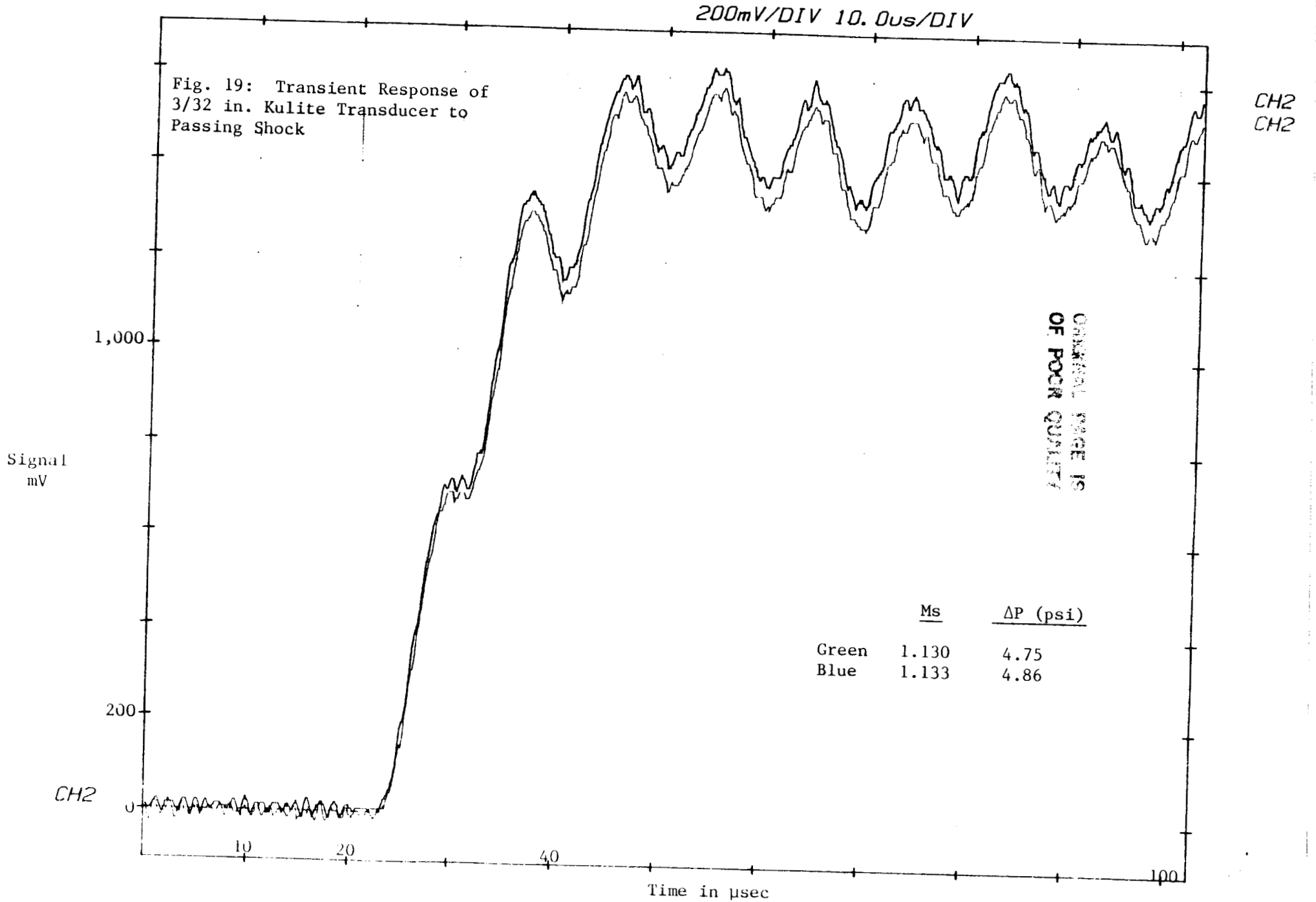

Fig. 19: Transient Response of 3/32 in. Kulite Transducer to Passing Shock

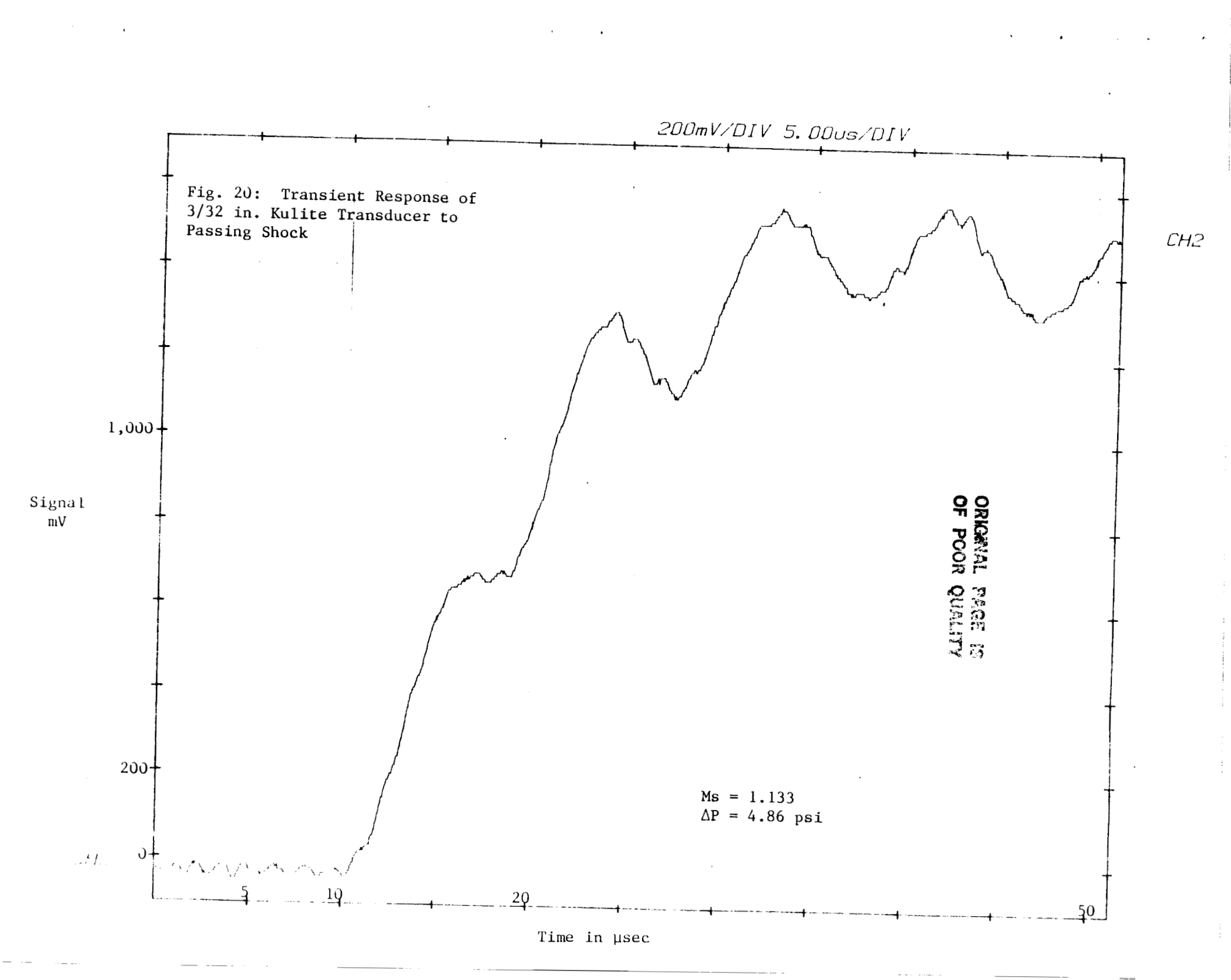

Fig. 20: Transient Response of 3/32 in. Kulite Transducer to Passing Shock

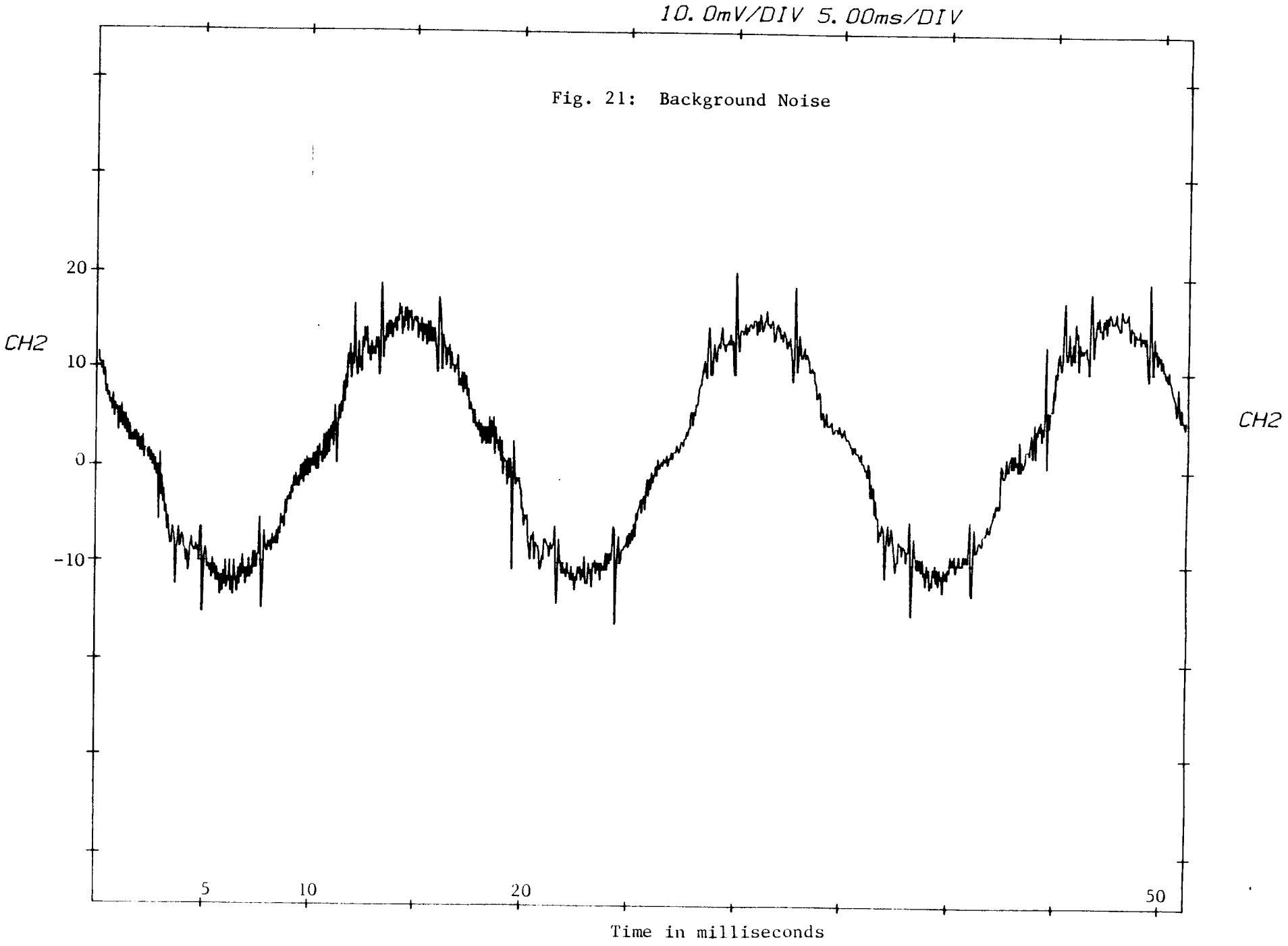

Fig. 21: Background Noise